

SCUBA observations of MAMBO sources

Steve Eales^{1*}, Frank Bertoldi², Rob Ivison³, Chris Carilli⁴,
Loretta Dunne¹ and Frazer Owen⁴

¹ *Department of Physics and Astronomy, Cardiff University, P.O. Box 913, Cardiff CF2 3YB, UK*

² *Max-Planck-Institut für Radioastronomie, Auf dem Hügel 69, 53121 Bonn, Germany*

³ *Astronomy Technology Centre, Royal Observatory, Blackford Hill, Edinburgh EH9 3HJ, UK*

⁴ *NRAO, Socorro, NM 87801, USA*

17 November 2018

ABSTRACT

We have observed 23 sources from the MAMBO 1200 μm survey with SCUBA at 850 μm , detecting 19 of the sources. The sources generally have low values for the ratio of 850 μm to 1200 μm flux. Two possible explanations for the low values are either that the sources are at very high redshifts or that the global properties of the dust in the MAMBO sources are different from the global properties of dust in low-redshift galaxies. If the former explanation is correct, we estimate that 15 of the MAMBO sources lie at $z > 3$.

Key words: submillimetre-dust-galaxies:evolution-galaxies:formation

1 INTRODUCTION

The luminous high-redshift dust sources discovered by the SCUBA submillimetre and MAMBO millimetre surveys (Smail, Ivison & Blain 1997; Hughes et al. 1998; Barger et al. 1998; Eales et al. 1999; Bertoldi et al. 2000,2001) are of great significance for our understanding of galaxy formation. The ultimate energy source in these objects is hidden by dust but the two obvious possibilities are that (1) the dust is being heated by a hidden active nucleus or (2) the dust is being heated by a luminous population of stars. The first of these possibilities can now largely be ruled out because of the failure of the XMM/Newton and Chandra telescopes to detect strong X-ray emission from many of the dust sources (e.g. Almaini et al. 2003; Waskett et al. 2003). Estimates of the star-formation rates necessary to produce the dust luminosity can be as high as $6 \times 10^3 M_{\odot}$ (Smail et al. 2003), enough to produce the stellar population of a massive galaxy in $\sim 10^8 - 10^9$ years. Many authors have concluded that these dust sources are the ancestors of present-day elliptical galaxies, basing their arguments on estimates of the star-formation rate in the population as a whole (Smail, Ivison and Blain 1997; Hughes et al. 1998; Blain et al. 1999), on estimates of the contribution of the sources to the extragalactic background radiation (Eales et al. 1999), and on comparisons of the space-density of the SCUBA/MAMBO sources (henceforth SMS) with the space-density of ellipticals in the universe today (Scott et al. 2002; Dunne, Eales and Edmunds 2003).

We are still, however, remarkably ignorant about this population. A major problem has been the lack of accurate redshifts for the SMSs. The practical difficulties here are the large errors on the positions of the SMSs, which often make it difficult to determine the optical/IR counterpart to the SMS, and the faintness of these counterparts, which make it difficult to measure an optical spectroscopic redshift. Until recently, the recourse of most groups has been to *estimate* the redshifts from the ratio of radio to submillimetre flux. The surface density of radio sources in deep VLA radio surveys is low enough that it is possible to be confident that apparent radio counterparts to SMSs are not chance coincidences. About 50% of the SMSs are also faint radio sources (Smail et al. 2000; Ivison et al. 2002; Clements et al. 2003). The discovery that a large fraction of SMSs are radio sources is extremely useful, because for these SMSs it is then possible, because of the accurate radio positions, to determine the optical/IR counterpart to the SMS. Furthermore, Carilli and Yun (1999) pointed out that, if SMSs are star-forming galaxies like those in the universe today, it is possible to estimate the redshift of the SMS from the ratio of radio to submillimetre flux.

Recently, however, Chapman et al. (2003) have taken a major step forward by measuring the redshifts for a significant number of SMSs. Rather surprisingly, given the dust in these objects, this group succeeded in detecting Lyman α and other *UV* lines with the Keck Telescope in 10 radio-selected SMSs. The redshifts they have measured lie in the range $0.8 < z < 4$ with an interquartile range of $1.9 < z < 2.8$, although this distribution may be skewed towards low red-

* E-mail: sae@astro.cf.ac.uk

shifts because of the requirement that the SMSs be detected at radio wavelengths.

A less widely-appreciated problem is the unknown temperature of the dust in the SMSs. The strong dependence of bolometric luminosity on dust temperature means that estimates of the star-formation rates, both of individual objects and of the population as a whole, are extremely uncertain. To our knowledge, there is no SMS without a powerful active nucleus which has a sufficiently well-sampled spectral energy distribution to permit an accurate estimate of the dust temperature. This is a fundamental problem because although the SMSs are often assumed to be similar to the Ultraluminous Infrared Galaxies in the nearby universe, the constraints on the spectral energy distributions are consistent with the SMSs being much colder and less luminous than ULIRGs (Eales et al. 2000; Efstathiou and Rowan-Robinson 2003). These first two problems are connected. Because of the degeneracy between dust temperature and redshift (Blain 1999), it is impossible to make an accurate estimate of the dust temperature without first measuring the redshift.

A third problem is simply the uncertain reliability of submillimetre and millimetre surveys. The efficiency of submillimetre surveys with SCUBA and MAMBO is extremely low, requiring typically eight hours of observations to produce a single SMS. Something that is again not widely appreciated is that if these instruments had been only a factor of two less sensitive virtually no SMSs would have been detected. These facts mean that most SMSs are quite close to the detection limits of the surveys, and low signal-to-noise combined with highly confused fields lead to interesting problems in data analysis. Different groups have adopted different data-reduction procedures, and there has been much vigorous debate within the community about the reliability of the different procedures and about the fraction of SMSs which are likely to be genuine.

In this paper we present SCUBA observations at $850\mu\text{m}$ of a sample of sources from a survey with MAMBO at $1200\mu\text{m}$. There were two motives for our programme. The first was to provide a simple cross-check between the surveys. Are the SMSs detected by MAMBO confirmed by our SCUBA observations? Are the ratios of $850\mu\text{m}$ to $1200\mu\text{m}$ flux what one would expect for star-forming galaxies at high redshift? The second motive was to use this ratio to determine whether there is a population of SMSs at very high redshift; at high redshifts this ratio falls as the wavelengths probed move, in the rest frame of the source, towards the peak of the dust spectral energy distribution. We assume a value for the Hubble constant of $75 \text{ km s}^{-1} \text{ Mpc}^{-1}$.

2 THE MAMBO SAMPLE

The Max-Planck Millimeter Bolometer array (MAMBO, Kreysa et al. 1998) on the IRAM 30m telescope has been used to carry out the first survey of the sky at millimetre wavelengths. The survey is being carried out in three main fields: the Lockman Hole, the NTT Deep Field, and a field centred on the cluster Abell 2125. The survey has already discovered roughly the same number of dust sources as have been found in the surveys with SCUBA at $850\mu\text{m}$. Some pre-

liminary results from the survey were presented by Bertoldi et al. (2000,2001) and Dannebauer et al. (2002).

We produced a sample of MAMBO sources to observe with SCUBA by selecting all sources in the MAMBO catalogue (as of mid 2001) with S/N greater than four and then imposing a lower flux limit of 3.3 mJy in the NTT field and 3 mJy in the other two fields. In the NTT field there are eight sources which met these criteria. We observed seven of these with SCUBA and also one other source (NTT-MM22) which falls slightly below our flux limit. In the Abell 2125 field there are 19 sources which met our criteria. We observed ten of these and also one other source (Abell2125-MM50) which falls slightly below our flux limit. In the Lockman Hole field there are six sources which met our selection criteria. We observed two of these sources, and two other sources (LH-MM34 and LH-MM8) fall within the area surveyed at $850\mu\text{m}$ as part of the SCUBA 8mJy survey (Scott et al. 2002).

Although we have observed almost all the sources in the NTT sample, we have failed to observe (through pressure of observing time) a significant fraction of the sources in the other two samples. The sample of sources which we did observe is biased in one important respect. Our SCUBA observations (§3) were made in photometry mode, in which a single bolometer is pointed at the target position. For these observations to be reliable, accurate positions are clearly essential. We therefore gave precedence to sources with accurate positions, either from observations with the Plateau de Bure millimetre interferometer (Dannebauer et al. 2002) or from VLA radio observations. Our bias towards sources with VLA detections (only one of the sources in our statistically-complete MAMBO samples which we did not observe with SCUBA was definitely detected by the VLA) creates a potential redshift bias in our project. The ratio of radio to millimetre flux is expected to decrease with redshift (Carilli and Yun 1999), and so the sample of MAMBO sources we observed with SCUBA may be biased towards low redshifts. We estimate, from the predicted relationship between the radio/submillimetre ratio and redshift (§6), that the MAMBO sources which were not detected by the VLA lie mostly at $z > 3$.

Table 1 lists all the sources we observed. The position given for each source is the position we used for the SCUBA photometry. In order of preference, we used the Plateau de Bure position, the VLA position or the original position found in the MAMBO survey. For the sources for which we used the VLA position, we have also given our estimate of the probability that the VLA source is not actually associated with the MAMBO source. This is given by $p = 1 - \exp(-n\pi d^2)$, in which d is the angular distance between the MAMBO source and radio source and n is the surface density of radio sources on the sky, which we calculated using the 1.4 GHz source counts given in Richards (2000).

3 SCUBA AND NEW MAMBO OBSERVATIONS

The SCUBA submillimetre camera on the James Clerk Maxwell Telescope is described in detail in Holland et al. (1999). It consists of two arrays: an array of 91 bolometers for operation at short wavelengths, usually $450\mu\text{m}$, and an

Table 1. The Sample

(1) Name	(2) S _{1200μm} /mJy	(3) Position (2000.0)	(4) Type	(5) 1.4-GHz flux/ μ Jy	(6) Radio ref.	(7) d/arcsec	(8) P(radio)
LH-MM13	4.2 \pm 1.0	10 52 01.05 57 24 46.10	R	73 \pm 10	I	7.6	0.055
LH-MM86	4.6 \pm 0.6	10 52 14.18 57 33 28.3	R	74 \pm 8	B	1.0	9.6 \times 10 ⁻⁴
NTT-MM3	4.6 \pm 1.0	12 05 08.13 -07 48 11.8	R	88 \pm 15	B	2.1	0.0043
NTT-MM34	3.3 \pm 0.7	12 05 09.75 -07 40 02.5	M	< 50	B
NTT-MM25 ^a	4.3 \pm 0.6	12 05 17.93 -07 43 06.9	M	< 45	B
		12 05 17.59 -07 43 11.5	P	< 45	B
NTT-MM5	5.4 \pm 0.8	12 05 18.15 -07 48 04.4	M	< 45	B
NTT-MM1	5.2 \pm 1.0	12 05 19.87 -07 49 35.8	R	73 \pm 15	B	2.2	0.0046
NTT-MM16	3.4 \pm 0.7	12 05 39.47 -07 45 27.0	P	56 \pm 15	B	1.9	0.033
NTT-MM31 ^b	6.5 \pm 0.9	12 05 46.54 -07 41 32.9	R	44 \pm 15	B	0.1	7.8 \times 10 ⁻⁶
NTT-MM22	3.0 \pm 0.7	12 05 43.89 -07 43 31.3	M	< 45	B
A2125-MM2	4.2 \pm 0.7	15 39 58.10 66 13 35.9	R	313 \pm 8	O	2.1	0.0041
A2125-MM11	3.1 \pm 0.7	15 40 47.19 66 15 51.8	R	108 \pm 8	O	1.4	0.0018
A2125-MM13 ^c	3.6 \pm 0.7	15 40 49.42 66 20 15.1	R	71 \pm 8	O	4.5	0.019
A2125-MM21	4.6 \pm 0.7	15 41 17.85 66 22 33.7	R	141 \pm 8	O	2.7	0.0069
A2125-MM26	4.3 \pm 0.7	15 41 26.9 66 14 37.3	R	86 \pm 8	O	0.61	0.00035
A2125-MM27	4.9 \pm 0.6	15 41 27.29 66 16 17.0	R	67 \pm 8	O	2.9	0.0077
A2125-MM28	3.9 \pm 0.7	15 41 28.78 66 22 02.7	R	1332 \pm 8	O	4.5	0.019
A2125-MM42	3.1 \pm 0.7	15 42 10.66 66 21 13.0	R	175 \pm 8	O	3.0	0.0082
A2125-MM50	4.6 \pm 1.3	15 42 20.27 66 07 16.0	R	103 \pm 8	O	4.9	0.023
A2125-MM32	4.2 \pm 1.0	15 41 42.83 66 05 59.0	R	89 \pm 8	O	0.5	0.00025
A2125-MM29	3.3 \pm 0.7	15 41 38.18 66 08 01.2	M	< 30	O

(1) Galaxy name; (2) flux at 1200 μ m measured in the MAMBO survey; (3) position (RA and Dec, J2000.0) used for the SCUBA observation; (4) provenance of position: M indicates a position from the original MAMBO survey, R indicates a VLA position, P indicates a position measured with the IRAM Plateau De Bure interferometer; (5) radio flux at 1.4 GHz in μ Jy; (6) reference for radio map: I—Ivison et al. (2002); B—Bertoldi et al. (2003); O—Owen et al. (2003); (7) the distance in arcsec from the MAMBO position to the radio position; (8) the probability that the radio source is not associated with the MAMBO source.

Notes: a—see Section 4 for a description of the astrometry for this source. b—the position given here is the radio position, which we used for the SCUBA observation; the position measured by the Plateau de Bure interferometer (12 05 46.59 -07 41 34.3) is only 1.6 arcsec away, much less than the size of the SCUBA beam. c—There are two radio sources close to the MAMBO position, one 0.8 arcsec from the MAMBO position and one 4.5 arcsec from the MAMBO position. The probability of either being chance associations is low (0.06% and 1.9%). This is not unusual for SMSs (Ivison et al. 2002) and is probably due to both radio sources being associated in some way, possibly being in the same cluster. The radio source which is most likely to be physically associated with the SMS is the closer one, and this is the position we used for our MAMBO on-off observation (15 40 50.01, 66 20 15.1). However, by mistake we observed the other position with SCUBA (the position given above). Fortunately, the difference between the two positions (3.55 arcsec) is much less than the size of the SCUBA beam. We estimate, from the shape of the SCUBA beam at 850 μ m, that our 850 μ m measurement should be lower than the true value by \simeq 20%. In calculating the ratio of 850 μ m to 1200 μ m flux, we have therefore increased the 850 μ m flux given in Table 2 by this factor.

array of 37 bolometers for use at long wavelengths, usually 850 μ m; a dichroic beamsplitter is used to simultaneously observe the same field at the two wavelengths. The beam size is about 8 arcsec and 14 arcsec (full-width half-maximum) at 450 and 850 μ m.

We observed the MAMBO sources in photometry mode, in which a single bolometer in each array is pointed at the target. During the commissioning of SCUBA it was discovered that the best photometric accuracy is obtained by averaging the signal over an area slightly larger than the beam size. To achieve this, the secondary mirror is ‘jiggled’ so that the bolometer samples a 3 by 3 grid with a grid spacing of 2 arcsec. This was the procedure we followed. We also chopped and nodded the secondary mirror in the standard way, using a chop throw of 60 arcsec. Before observing the MAMBO source, we observed a standard JCMT pointing source close to the MAMBO source and chosen to be on the same side of the meridian, since the pointing and tracking accuracy of the JCMT deteriorates as the telescope moves across the meridian. During each night we monitored the opacity of the

atmosphere at both 450 and 850 μ m using ‘skydips’ and we determined the flux calibration from observations of one or more of the standard JCMT flux calibrators. Our observations were carried out on 14 separate nights from May 2001 until February 2002. The dates on which the sources were observed, the integration times, and the typical opacity of the atmosphere during the observations are listed in Table 2.

We reduced the data in the standard way using the SURF package (Jenness 1997). We first subtracted the signals recorded in the two nods from each other, and then divided the result by the array’s flat-field. We then corrected the result for the opacity of the atmosphere, interpolating between the results from the skydips to determine the opacity of the atmosphere at the time of the observation. Even with chopping and nodding, and even in the best conditions, there is usually some residual sky signal visible on the SCUBA images. Fortunately, this residual signal, although variable with time, does not vary much across the arrays, and so the signal in the bolometers which are not pointing

towards the target can be used to removed the remaining sky signal. We made this correction, for each second of data, by subtracting the median of the signals recorded by the redundant bolometers from the signal recorded by the bolometer pointed at the target.

The result of this procedure is a plot of intensity verses time for the target bolometer from which all instrumental and atmospheric effects have been removed. Each point on the plot corresponds to one second of data. As the final step in the data reduction, we removed all points more than 3σ away from the mean and then took the mean of the remaining points as our estimate of the intensity.

The $850\mu\text{m}$ results are listed in Table 2. The flux errors were calculated by adding in quadrature the error obtained from the scatter on the intensity-verses-time plot and the photometric error obtained from the observations of flux calibrators. SCUBA data at $850\mu\text{m}$ is remarkably photometrically stable, and our estimates of the photometric error were $\approx 5\text{--}10\%$. As can be seen from the table, we observed about half the sample on at least two different nights. Except in one case (A2125-MM26), the values measured on the different nights were consistent. The final flux value for each source is a weighted average of the results for the different nights. Our photometric measurement for LH-MM13 agrees well with that measured from a SCUBA map by Scott et al. (2002).

At $450\mu\text{m}$, we detected only two objects at greater than the 3σ level. We detected A2125-MM28 with a S/N of 6.5 and A2125-MM11 with a S/N of 3.2. Unfortunately, because of the greater difficulties of calibrating $450\mu\text{m}$ data (Dunne and Eales 2001), the calibration uncertainties are very large for these two objects. With these calibration uncertainties, we estimate the $450\mu\text{m}$ flux of the first source as $26 \pm 14\text{mJy}$ and the $450\mu\text{m}$ flux of the second source as $19 \pm 11\text{mJy}$.

In addition to the SCUBA observations, we used the MAMBO array to make new flux measurements at $1200\mu\text{m}$ of 14 of the sources in Table 1. The aims of this were (1) to check the fluxes obtained from the MAMBO survey and (2) by carrying out the MAMBO photometry at the same position used for the SCUBA photometry, to minimise the effect of astrometric errors on our estimates of the $850\mu\text{m}$ to $1200\mu\text{m}$ flux ratio. We used the MAMBO ‘on-off’ mode, which is equivalent to the SCUBA photometry mode. We reduced the data using a similar procedure to that used for the SCUBA photometry. The new MAMBO fluxes are given in the last column in Table 2.

4 NOTES ON INDIVIDUAL SOURCES

In this section we give notes, when appropriate, on individual sources:

LH-MM13: There is a large offset (7.6 arcsec) between the positions of the MAMBO source and the VLA radio source, much the largest for our sample of MAMBO sources (§5.2), although the statistical analysis shows that the probability this is a chance association is only 6%. This source is in the region mapped with SCUBA at $850\mu\text{m}$ by Scott et al. (2002). The brightest source in their survey, L850.1, is much closer (3.0 arcsec) to the radio source. This positional disagreement has recently been resolved by a new MAMBO map, which shows the position of the MAMBO source is quite close to

the radio and SCUBA positions. The initial disagreement is thought to have been caused by the effect of a large value for the noise close to the edge of the original MAMBO map (Bertoldi, private communication). The position we used for our SCUBA and MAMBO photometry is that of the radio source. Our $850\mu\text{m}$ measurement and that of Scott et al. agree well.

LH-MM34 and **LH-MM8:** We did not observe these MAMBO sources with SCUBA, but they fall in the region mapped with SCUBA by Scott et al. (2002). The positions of the SCUBA sources L850.14 and L850.2, whose fluxes we give in Table 2, agree well with the positions of the two MAMBO sources.

NTT-MM25: The positions given in Table 1 are the original MAMBO position and the position of the source detected with the Plateau de Bure interferometer at $1260\mu\text{m}$ by Dannebauer et al. (2002). The positions are separated by 6.8 arcsec. The obvious inference to draw from this would be that the original MAMBO position was substantially in error. However, we detected much stronger $850\mu\text{m}$ emission at the original MAMBO position than at the position measured by the interferometer. Recent new data taken with the interferometer, when added to the original data, has produced a new position for the SMS (12 05 17.86, -07 43 08.5), which is only 1.9 arcsec away from the original survey position (Bertoldi, private communication). When calculating the ratio of $850\mu\text{m}$ and $1200\mu\text{m}$ flux for this source, we used the SCUBA and MAMBO on-off measurement at the original survey position.

5 A COMPARISON OF THE SCUBA AND MAMBO RESULTS

A basic result of our SCUBA observations is that most of the 4σ sources detected by the MAMBO survey are real. Of the 23 MAMBO sources for which there are SCUBA observations, only four were not detected at $> 3\sigma$ with SCUBA. Of these four, one was detected by SCUBA at 2.9σ and one other was detected by the VLA. Therefore, of the 23 MAMBO sources, there are only two for which there is not corroborating evidence in another waveband. In this section, we will use our new datasets to investigate some of the basic characteristics of the SCUBA and MAMBO surveys. We will first use our new MAMBO photometry to investigate the issue of flux-boosting. We will then use the radio and MAMBO datasets to investigate the astrometric accuracy of the MAMBO survey. Finally, we will start to compare the fluxes measured for individual SMSs by MAMBO and by SCUBA.

5.1 Flux Boosting

Several groups (Hogg 2001; Eales et al. 2000; Scott et al. 2002) have argued that ‘flux-boosting’ will be important in submillimetre and millimetre surveys. Flux boosting is an effect which may occur in any magnitude- or flux-limited sample of sources. If the differential source counts decrease with flux density, a source in the final sample is more likely to have had its flux density enhanced than depressed by the effect of noise. Flux boosting is a particular example of the

Table 2. Photometry

(1) Name	(2) Date	(3) Int. time (s)	(4) $\tau_{850\mu\text{m}}$	(5) $S_{850\mu\text{m}}$ (mJy)	(6) S/N	(7) other $S_{850\mu\text{m}}$ (mJy)	(8) $S_{1200\mu\text{m}}$ /mJy (survey)	(9) $S_{1200\mu\text{m}}$ /mJy (on-off)
LH-MM13 [†]	20020216	5400	0.21	8.7 ± 1.8	5.7	10.5 ± 1.6	4.2 ± 1.0	3.5 ± 0.5
	20020218	1260	0.13	11.0 ± 2.8	4.2
				9.4 ± 1.5	7.1
LH-MM34 [†]				9.5 ± 2.8	3.3 ± 0.7	...
LH-MM8 [†]				10.9 ± 2.4	4.6 ± 0.8	...
LH-MM86	20011224	1800	0.34	15.0 ± 3.0	5.8	...	4.6 ± 0.6	...
NTT-MM3	20020207	1800	0.24	7.0 ± 2.6	2.8	...	4.6 ± 1.0	3.2 ± 1.0
	20020208	4770	0.24	5.9 ± 1.3	4.9
				6.1 ± 1.2	5.6
NTT-MM34	20020222	1800	0.25	1.8 ± 2.3	0.8	...	3.3 ± 0.7	3.8 ± 1.7
	20020223	3600	0.22	-1.4 ± 1.8	-0.8
				-0.2 ± 1.4	-0.1
NTT-MM25M [†]	20020222	5400	0.24	5.7 ± 1.5	4.3	...	4.3 ± 0.6	3.0 ± 0.5
	20010514	3600	0.27	7.7 ± 1.6	5.5
	20020218	5400	0.16	5.3 ± 1.9	2.9
				6.3 ± 0.9	7.5
NTT-MM25P [†]	20020211	3600	0.30	0.4 ± 2.1	0.2	2.7 ± 0.8
NTT-MM5	20010521	6120	0.30	5.9 ± 2.2	2.9	...	5.4 ± 0.8	2.2 ± 1.9
	20020211	3600	0.36	7.3 ± 2.0	3.8
				6.7 ± 1.5	4.8
NTT-MM1	20020208	3600	0.22	5.5 ± 1.6	3.7	...	5.2 ± 1.0	5.3 ± 1.0
	20020209	3150	0.17	3.5 ± 1.6	2.2
				4.5 ± 1.2	4.3
NTT-MM16	20020207	6858	0.24	6.3 ± 1.4	5.3	...	3.4 ± 0.7	3.8 ± 1.0
NTT-MM31	20010514	3600	0.33	18.5 ± 2.4	12.7	...	6.5 ± 0.9	10.6 ± 1.0
NTT-MM22	20010522	5760	0.29	2.3 ± 1.4	1.6	...	3.0 ± 0.7	...
A2125-MM2	20020208	7200	0.23	5.9 ± 1.3	4.9	...	4.2 ± 0.7	...
A2125-MM11	20010522	6660		2.1 ± 1.6	1.3	...	3.1 ± 0.7	3.1 ± 0.57
	20011223	3600	0.16	3.9 ± 1.4	2.9
				3.1 ± 1.1	3.2
A2125-MM13 ^a	20020207	6300	0.30	4.9 ± 1.6	3.3	...	3.6 ± 0.7	2.5 ± 0.9
	20020209	2196	0.21	8.5 ± 2.6	3.4
				5.9 ± 1.4	4.7
A2125-MM21	20010520	5580	0.44	11.7 ± 2.8	5.4	...	4.6 ± 0.7	6.0 ± 1.3
	20020211	4500	0.32	12.4 ± 2.4	5.9
				12.1 ± 1.8	8.0
A2125-MM26	20010305	4320	0.17	8.5 ± 1.4	7.6	...	4.3 ± 0.7	4.0 ± 0.5
	20010514	2880	0.23	16.8 ± 2.3	10.8
				10.7 ± 1.2	13.2
A2125-MM27	20010305	4320	0.17	14.6 ± 1.8	13.3	...	4.9 ± 0.6	4.2 ± 0.3
A2125-MM28	20011223	4500	0.14	5.8 ± 1.2	5.5	...	3.9 ± 0.7	2.8 ± 0.9
A2125-MM42	20020222	2160	0.36	0.4 ± 2.5	0.2	...	3.1 ± 0.7	...
	20020223	3240	0.19	5.8 ± 2.1	2.9
				3.6 ± 1.6	2.9
A2125-MM50	20020223	5400	0.18	6.5 ± 1.6	4.3	...	4.6 ± 1.3	...
A2125-MM32	20020222	5400	0.24	6.00 ± 1.6	4.1	...	4.2 ± 1.0	...
A2125-MM29	20020211	3600	0.33	-2.6 ± 2.2	-1.2	...	3.3 ± 0.7	...

(1) Galaxy name. A dagger indicates there is a note on this source in Section 4; (2) date on which the observation was made; (3) integration time in seconds—this includes the time spent at the reference position; (4) optical depth of the atmosphere at $850\mu\text{m}$ during the observation; (5) flux at $850\mu\text{m}$ in mJy measured from this observation. The measurement in bold type is the weighted average of the individual measurements for this source. (6) signal-to-noise of observation; (7) flux measurement at $850\mu\text{m}$ for this object from Scott et al. (2002); (8) flux measurement at $1200\mu\text{m}$ in mJy from MAMBO survey; (9) flux measurement at $1200\mu\text{m}$ in mJy from subsequent MAMBO on-off observations. Notes: a—see note on this source in Table 1.

process described by Eddington (1940), in which the statistical properties of a a distribution of experimental measurements are distorted by noise. In the MAMBO and SCUBA surveys, there are two components to the noise: the noise arising from the experimental setup (instrumental and at-

mospheric) and the confusion noise arising from the SMSs which are too faint to be detected individually. Eales et al. (2000) carried out a Monte-Carlo simulation of their $850\mu\text{m}$ SCUBA survey, concluding that the average boosting factor is $\simeq 44\%$. Scott et al. (2002) carried out a Monte-Carlo sim-

ulation of their ‘8 mJy’ SCUBA survey, concluding that for this survey the boost factor is $\simeq 15\%$.

We can address the question of flux boosting in the MAMBO survey empirically using our new MAMBO photometry. If an SMS was boosted into the original MAMBO survey by noise, the new flux should be lower than the original survey flux. This is strictly true only for the first type of noise; as long as the direction and size of the chop throw used in the photometry and the original survey were the same, the two fluxes will have been affected by the confusion of faint sources in the same way. We can therefore only set a lower limit on the flux boosting factor. The positions from the MAMBO survey will, of course, have been affected by both instrumental noise and the confusion of faint sources, but since our photometric observations were almost always made at the accurate radio positions, this should not be a serious issue.

Figure 1 shows the ratio of the $1200\mu\text{m}$ fluxes measured from the survey and from the photometry plotted against the survey flux. We have also plotted the results of a Monte-Carlo simulation of the MAMBO survey (§7). Inspection of Table 2 shows that there is only one SMS for which the MAMBO survey flux and the MAMBO photometric flux are significantly different, and the general good agreement is evidence that fluxes measured with MAMBO are reproducible. In the figure, the effect of flux boosting can be clearly seen in the Monte-Carlo simulation, but is less clear in the real data. Excluding the one SMS with a big difference between the two fluxes and one SMS which was detected with low signal-to-noise in the photometry, the average ratio of the survey flux density to the photometric flux density is 1.14 ± 0.07 . This is slightly lower than the flux-boosting factors inferred for the SCUBA surveys, although our estimate for the MAMBO survey is strictly only a lower limit. The difference might also be explained by the smaller beam of the MAMBO survey (11 arcsec) compared with the SCUBA surveys (14 arcsec).

5.2 The accuracy of the MAMBO positions

Many authors have tried to quantify the positional accuracy of submillimetre and millimetre surveys using Monte-Carlo simulations (e.g. Eales et al. 2000; Hogg 2001; Scott et al. 2002). We can address this question empirically for the MAMBO survey using the differences between the positions from the survey and the accurate positions (measured either with the VLA or the Plateau de Bure interferometer). Figure 2 shows a histogram of these differences. The median difference is 2.0 arcsec, fairly modest given the size of the MAMBO beam (FWHM of 11 arcsec). Nevertheless, there are a few SMSs with large offsets, suggesting that the effect of source confusion may sometimes be important.

5.3 A Comparison of the MAMBO and SCUBA Fluxes

The ratios of $850\mu\text{m}$ and $1200\mu\text{m}$ flux for the SMSs in our sample are much lower than expected for a low-redshift galaxy. The explanation of this difference may either be astrophysical (the SMSs are either at higher redshifts or have different rest-frame spectral energy distributions to galaxies

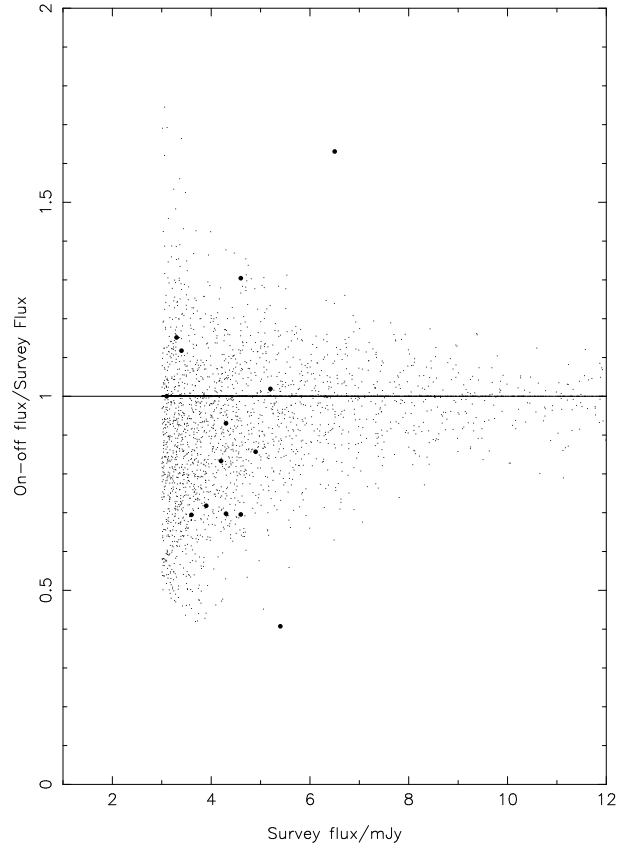


Figure 1. The large symbols show the ratio of the $1200\mu\text{m}$ flux measured using the MAMBO photometry (‘on-off’) mode to the flux measured by the survey, plotted against the survey flux. The small points show the results from the Monte-Carlo simulation of the MAMBO survey described in §7. For these points the quantity plotted on the y-axis is the ratio of the $1200\mu\text{m}$ flux in the absence of noise to the flux after noise has been added. The quantity plotted on the x-axis is the flux after noise has been added. Only sources which would have been detected in the survey have been plotted.

at low redshift) or there might be some systematic error as the result of our experimental method. In this section we will consider the latter possibility.

An obvious possibility is that there is an error in the absolute flux calibration of one of the telescopes. However, the primary flux calibrators of both telescopes are the same objects: the planets Mars, Uranus and Neptune. Moreover, the sets of secondary calibrators for both telescopes (used when a planet is not visible) have a large overlap (Sandell 1994; Lisenfeld et al. 2000). Lisenfeld et al. have compared the fluxes of 11 secondary calibrators measured at a similar wavelength with the IRAM 30-metre and the JCMT, finding that the ratio of JCMT-to-IRAM flux has an average value of 0.99 with a standard deviation of 0.13. Thus, it seems certain that the low values of the 850 to $1200\mu\text{m}$ flux ratio are not caused by an error in the absolute flux calibration.

A second effect to consider is the effect of bandwidth. The filter used in the SCUBA observations has a central frequency of 347 GHz and a bandwidth (FWHM) of 30 GHz. The spectral response of MAMBO is more complicated. Carilli et al. (2001) give the half-power sensitivity range as 210–290 GHz but note that the overall profile is asymmetric, with

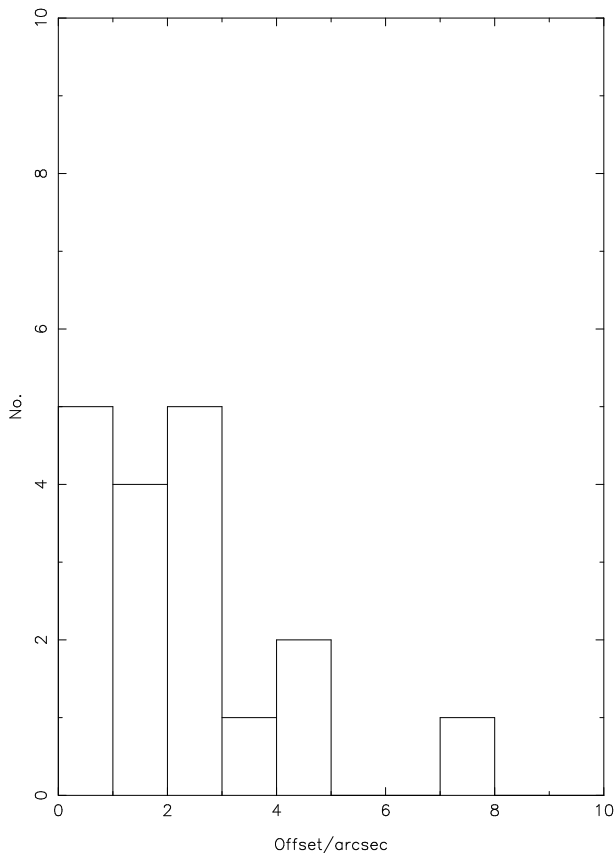


Figure 2. Difference between the position from the MAMBO survey and the position measured with the VLA or the Plateau de Bure interferometer.

a sharp rise in sensitivity at lower frequency, and then a gradual decrease in sensitivity to higher frequency. The instrumental spectral responses of both instruments should, in principle, be convolved with the transmission curve of the atmosphere, which will depend on the conditions in which a particular observation was made. We have made an estimate of the effect of the finite bandwidth by assuming that the spectral response for both instruments has the form of a top hat, with the width of the top hat being the measured FWHM. We have assumed that an SMS has a power-law spectral energy distribution ($S_\nu \propto \nu^\alpha$). For values of α of 1, 2, 3 and 4, our estimates of the values measured for the flux ratio through these filters are 1.39, 1.91, 2.61, and 3.54, respectively. Our estimates of the values that would be measured through filters of zero width are 1.39, 1.93, 2.67, and 3.71, respectively. Thus, it is only when the flux ratio is very large that the effect of bandwidth becomes important, and the measured values of the flux ratio of the MAMBO sources are generally much less than this.

The final issue we need to address are the effect of astrometric errors on the SCUBA $850\mu\text{m}$ photometry. Two types of astrometric errors might be important: (1) an error in the position assumed for the MAMBO source, (2) JCMT pointing/tracking errors. We can eliminate the first possibility easily, because for all but five of the 23 sources there is either an accurate position (from the VLA or the Plateau de Bure interferometer) or the $850\mu\text{m}$ flux was measured from a submillimetre map. For the remaining five sources we were

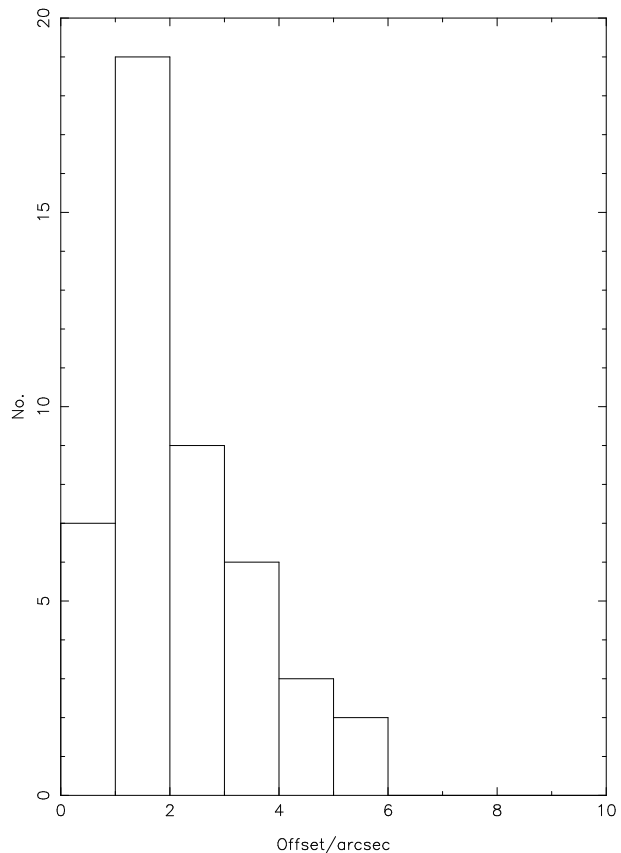


Figure 3. Difference between the actual and expected positions of the JCMT pointing source observed after the observation of the MAMBO source.

forced to use the MAMBO survey position but, as we showed in the previous section, these positions are quite accurate. The median error in Figure 2 (2 arcsec) is much less than the beam size of SCUBA (FWHM of 14 arcsec), and a pointing error of this size would lead to an underestimate of the true $850\mu\text{m}$ flux by only 6%.

We can investigate the effect of the second type of error using our JCMT dataset. We always observed a JCMT pointing source before, and in most cases after, observing the MAMBO source (§3). The difference between the actual and expected position of the second pointing source can be used to investigate the effects of tracking and pointing. Figure 3 shows a histogram of this difference for all observations in which the second pointing source was in the same part of the sky as the target. The median discrepancy is 1.91 arcsec.

The way this is interpreted depends on whether tracking or pointing errors are most important. Let us first suppose the positional discrepancies are caused by tracking errors. On the assumption that the tracking errors accumulate linearly with time, the average positional error during an observation will be about half that shown in the figure. The median positional error due to tracking problems is therefore 0.96 arcsec, which would lead to an underestimate of the true $850\mu\text{m}$ flux by $\simeq 1\%$. Now let us suppose that the discrepancies are caused by pointing errors. On the assumption that the pointing error on moving to the target and the pointing error on moving to the second pointing source add in quadrature, the median pointing error would be $1.91/\sqrt{2} = 1.35$

arcsec. An error of this size would lead to an underestimate of the $850\mu\text{m}$ flux by $\simeq 3\%$.

Therefore, we conclude that astrometric errors, of whichever kind, should have a relatively small effect on the $850\mu\text{m}$ fluxes. Furthermore, in calculating the ratio of the $850\mu\text{m}$ and $1200\mu\text{m}$ flux of an SMS we have used, where possible, the $1200\mu\text{m}$ flux measured from our follow-up photometry. Since this photometry was carried out at the same position and should have the same pointing/tracking concerns as the SCUBA photometry, for these SMSs there is no reason at all to expect astrometric errors to lead to an underestimate of the flux ratio.

6 ASTROPHYSICAL EXPLANATIONS OF THE LOW FLUX RATIOS

Figure 4 shows a comparison of the $850/1200\mu\text{m}$ flux ratios of the MAMBO sources with the flux ratios of dust sources of known redshift. The spectral energy distributions of high-redshift SMSs are very poorly known. In a search through the literature, we were unable to find a single high-redshift SMS without an obvious active nucleus which had a sufficiently well-sampled spectral energy distribution (SED) for a dust temperature to be determined. Some SMSs have been observed at several submillimetre wavelengths (Dey et al. 1999; Ivison et al. 2000), but not at a short enough wavelength in the rest-frame to sample properly the peak of the SED, the crucial part of the SED for determining the temperature of the dust. Our set of comparison dust sources in the figure are a sample of quasars observed both with MAMBO and with SCUBA (Omont et al. 2001; Isaak et al. 2002), a combined SCUBA-MAMBO dataset very similar to ours (an additional check that calibration differences are not an issue). The quasars are mostly at $z \sim 4$. We do not know the redshifts of the MAMBO sources, but if they are like the SCUBA sources observed by Chapman et al. (2003) they will lie in the redshift range $0.8 < z < 4$. In the figure we have plotted them at an arbitrary redshift of 0.2.

The values of the flux ratio for the MAMBO sources are generally lower than those for the quasars. There are two alternative explanations for this. As we show in detail below, the value of this flux ratio is expected to decline with redshift. Therefore, one possible explanation for the difference between the MAMBO sources and the quasars is that the MAMBO sources are generally at higher redshifts than the quasars. The alternative is that the rest-frame SEDs of the MAMBO sources are different than those of the quasars.

We have plotted in the figure the predicted relationship between the $850/1200\mu\text{m}$ flux ratio and redshift for various SEDs. The SED of a dust source is usually represented as

$$S_\nu = \nu^\beta \sum_i a_i B_\nu(T_i)$$

in which S_ν is the flux density at a frequency ν , B_ν is the Planck function and β is the dust emissivity index. The sum is over the components of dust at different temperatures, with a_i being the relative mass of the dust at a temperature T_i . The first set of predictions we have plotted in the figure are for a simple model in which there is only one dust component in a galaxy. We have plotted predictions based on

this model, for a number of temperatures and for two values of β .

The $850/1200\mu\text{m}$ flux ratios of the quasars are well-fitted by the predictions for SEDs with a single dust temperature and a value for β of 2. This conclusion is supported by more detailed investigations of the SEDs of high-redshift quasars. Priddey and McMahon (2002) find that the SEDs of high-redshift quasars can be well represented by dust at a single temperature with $\beta = 2$; Benford et al. (1999) find that the SEDs are fitted well by single-temperature dust with $\beta = 1.5$. If the rest-frame SEDs of the MAMBO sources can also be represented by dust at a single temperature with a high value of β , it is clear from the diagram that the MAMBO sources must generally be at higher redshifts than the quasars, and outside the range found by Chapman et al. (2003) for SCUBA sources.

However, observations of luminous low-redshift dust sources do not reveal SEDs like this. Dunne et al. (2000) and Blain, Barnard and Chapman (2003) have shown that the $850\mu\text{m}$ and IRAS far-infrared fluxes of low-redshift galaxies can be represented by dust at a single temperature. Dunne and Eales (2001—henceforth DE), however, have shown that when $450\mu\text{m}$ fluxes are added, it is often no longer possible to fit the fluxes with a single-temperature model. Furthermore, they have shown that the ratio of 450 and $850\mu\text{m}$ fluxes is remarkably constant over a wide range of galaxies types, from normal-looking spiral galaxies to ULIRGs such as Arp 220. The constancy and high value of this ratio require β to be close to two. With this value of β it is impossible to fit the fluxes with dust at a single temperature for virtually all galaxies. DE conclude that there are at least two dust components in nearby galaxies, with most of the dust being at $T_d \sim 20\text{K}$, even in the case of ULIRGs like Arp 220. Amure (2003) has reached the same conclusion with an independent dataset containing 15 spiral galaxies. Note, however, that this conclusion does not imply that all dust in a galaxy has a value for β of 2 or that there are only two dust components in a galaxy. Observations within the Galaxy have shown that the properties of dust depend strongly on environment (Dupac et al. 2002; Stepnik et al. 2003) and in reality there must be a range of dust temperatures. The DE conclusion is an empirical one: to fit the global submillimetre and far-infrared fluxes of nearby galaxies, it is necessary to use at least two dust components and a global value for β of 2. Priddey and McMahon (2002) have also reached the conclusion that the rest-frame SEDs of high-redshift quasars are different from those of low-redshift galaxies.

We estimated redshifts for the MAMBO sources in the following way, starting with the assumption that, in the rest frame, they are like the low-redshift galaxies modelled by DE. We first fitted the DE model to the submillimetre and far-infrared data for 104 galaxies in the IRAS Bright Galaxy Survey (DE; Dunne et al. 2000). We then used the model to predict how the $850/1200\mu\text{m}$ ratio should depend on redshift for each galaxy, taking proper account of the effects of the microwave background (Eales and Edmunds 1996). The thick line in Figure 4 shows the median predicted flux ratio at each redshift for the 104 galaxies, with the dashed lines showing the lowest and highest prediction.

We considered each MAMBO source in turn, determining the redshift at which each DE template produced the observed value of the $850/1200\mu\text{m}$ flux ratio. This produced

104 redshift estimates for each MAMBO source. We took the median of these redshift estimates as our estimate of the redshift for the MAMBO source. There are two sources of error on this estimate: (1) an error arising from the uncertainties in the 850 and 1200 μm fluxes, (2) an error arising from fact that a different template might be a better representation of the rest-frame SED of the MAMBO source. We estimated these errors separately. We estimated the first error using the DE template which had given the median redshift estimate. We allowed the redshift to vary in both directions until the Chi-square agreement between the predicted and observed fluxes (one degree of freedom) was sufficiently poor that the probability of it occurring by chance was 16%, effectively placing $\pm 1\sigma$ errors on the redshift estimate. We estimated the error from possibly using the wrong template in the following way. We ranked the 104 redshift estimates. The redshift estimate below which 16% of the estimates fell, and the redshift estimate above which 16% of the estimates fell, provided $\pm 1\sigma$ errors. We are, of course, making the assumption that the 104 templates represent the full range of SEDs of high-redshift SMSs. We added the two errors in quadrature. Table 3 lists the redshift estimates and the errors. In several cases we have given a lower or upper limit to the redshift. This is for galaxies where the observed value of the flux ratio fell either below the value predicted by the median template at all redshifts or above the value predicted by the median template at all redshifts. The limits are $\pm 1\sigma$ limits, in the sense that there is a probability of 16% that the true redshift is actually either below the lower limit given in the table or above the upper limit given in the table.

The errors on the redshift estimates are very large, mostly caused by the errors in the flux densities rather than by the diversity of possible templates, but in general the redshift estimates are very high. Fifteen out of 21 MAMBO sources for which there is corroborating evidence in other wavebands (§5) have redshifts estimated by this method of >3 .

Is there any obvious astrophysical way of avoiding this conclusion? One way to do this would be to alter the templates used to estimate the redshifts. If we assumed a single-temperature template with a value for β of 2, which reproduces the flux ratios of the quasars, it would actually make things worse, leading to even higher redshifts. A way to lower the redshift estimates, however, would be to use a single-temperature template with a value for β of 1. Figure 4 shows that the low values of the flux ratio might be explained by a low value for β with the MAMBO sources lying in the redshift range found by Chapman et al. (2003). If this is the case, the global properties of the dust in high-redshift SMSs must be different from those of dust in low-redshift galaxies.

In the absence of spectroscopic redshifts, the only other information about the redshifts of the MAMBO sources comes from the the ratio of radio and submillimetre flux, which, as Carilli and Yun (1999) originally pointed out, should be a function of redshift. Following the original suggestion, a number of groups used different samples of low-redshift objects to determine the expected relationship between the ratio of radio-to-submillimetre flux and redshift (Carilli and Yun 2000; Dunne, Clements and Eales 2000; Rengarajan and Takeuchi 2001). There are slight differ-

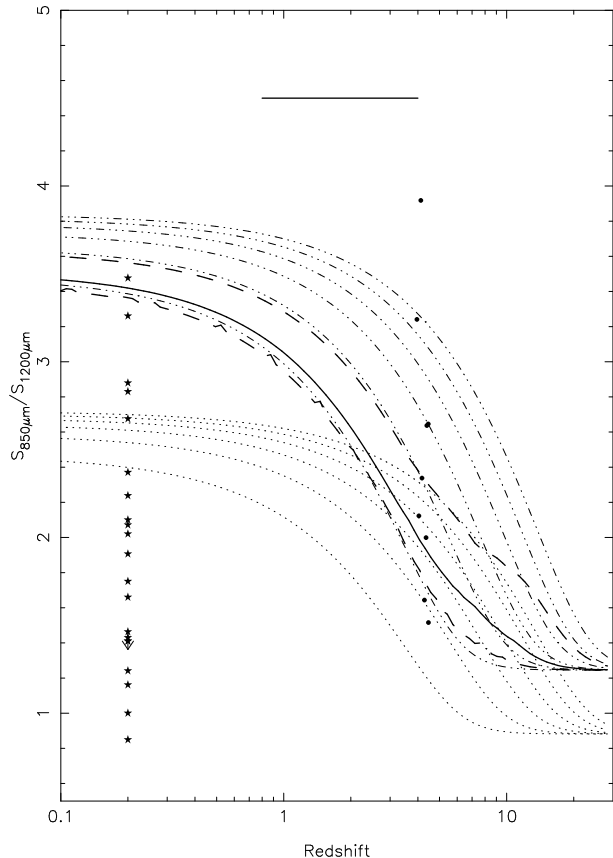


Figure 4. The ratio of $S_{850\mu\text{m}}$ and $S_{1200\mu\text{m}}$ flux versus redshift. The asterisks show the measured values of the flux ratio for the MAMBO sources (we omit the two sources for which there is no corroborating evidence in another waveband—§5). Since we do not know the redshifts of the MAMBO sources, we have plotted the points at an arbitrary redshift of 0.2. The dots show the values of the flux ratio for a sample of high-redshift quasars (Omont et al. 2001; Isaak et al. 2002). The horizontal line shows the range of spectroscopic redshifts for SCUBA sources found by Chapman et al. (2003). The thin lines show the relationship between flux ratio and redshift predicted for a single-temperature dust model, the dotted lines for $\beta = 1$, the dot-dashed lines for $\beta = 2$. For both sets, the lowest and highest lines are for dust temperatures of 20K and 70K, respectively, with the other lines being at an interval of 10K. The thick lines are predictions based on the models of Dunne and Eales (2001—see text). The continuous line shows the median predicted value of the flux ratio and the dashed lines show the lowest and highest predicted value at each redshift.

ences between the redshifts estimated using the different sets of low-redshift templates (Ivison et al. 2002), but for our work these differences are not important. We estimated a redshift for each MAMBO source using the observed ratio of radio-to-submillimetre flux or the limit on this ratio if the MAMBO source was not detected by the VLA. For low-redshift templates we used the 25 most radio-luminous sources from the sample of Dunne, Clements and Eales (2000), which produces very similar redshift estimates to using the templates in Carilli and Yun (2000). We used exactly the same method for estimating the redshift as we used to estimate the redshift from the 850/1200 μm flux ratio. As before, we estimated separately the errors arising from flux errors and from the range of possible templates, and then

added the errors in quadrature. We are of course assuming again that the templates represent the full range of SEDs of high-redshift SMSs. The results are shown in Table 3.

There are two obvious differences in the two sets of redshift estimates. First, the errors on the new set of redshift estimates are much smaller, mainly because the ratio of radio-to-submillimetre flux is a stronger function of redshift than the $850/1200\mu\text{m}$ flux ratio. Second, the redshifts estimated from the radio-to-submillimetre ratio are in general lower than those from the $850/1200\mu\text{m}$ flux ratio. Let us consider the number of sources with estimated redshifts > 3 . Using the radio method, there are six out of 21 sources with estimated redshifts > 3 , if we include sources which have redshift lower limits below three as being above this redshift. If we use the other method, there are 15 sources with estimated redshifts $z > 3$ (we assume that NTT-MM34 is at $z > 3$ because although we could not obtain a satisfactory fit to its $850\mu\text{m}$ and $1200\mu\text{m}$ fluxes, the very low value for the $850/1200\mu\text{m}$ ratio suggests a very high redshift). Therefore, although in the cases of individual sources the large errors on the redshift estimates often mean that the two redshift estimates are statistically consistent, there is a trend for the redshifts estimated using the radio method to be lower.

Is there any reason to conclude that one of the two methods is biased? We have no independent check on the redshifts estimated from the $850/1200\mu\text{m}$ flux ratio because there are virtually no SMSs with measurements of this flux ratio and spectroscopic redshifts. However, we can critically examine the second technique because there are now a significant number of SMSs with radio measurements and spectroscopic redshifts. Figure 5 shows the ratio of submillimetre to radio flux plotted against redshift for all SMSs which have both spectroscopic redshifts and radio measurements. Out of the 21 SMSs, 14 have positions which fall close to the positions predicted using low-redshift templates. Seven out of 21, however, fall a significant way from the predicted positions. The most interesting SMSs, from the point of view of this work, are the four which have much higher ratios of radio to submillimetre flux than the predicted values. One possible explanation of the excess radio emission is that these SMSs contain radio-emitting active nuclei. Therefore, one way to reconcile the two sets of redshift estimates in Table 3 would be if our MAMBO sample contains a large number of SMSs with radio-emitting active nuclei. The alternative way to reconcile the two sets of redshift estimates is to conclude that the radio estimates are correct and that the low values for the $850/1200\mu\text{m}$ flux ratio are caused by the rest-frame SEDs of the MAMBO sources being different from those of low-redshift galaxies.

To summarize the results of this section: The low $850\mu\text{m}/1200\mu\text{m}$ flux ratios of our sources may be explained by very high redshifts, although the redshifts estimated using the radio method are much lower. If the radio estimates are correct, the most likely explanation of the low flux ratios is that the global properties of dust in the MAMBO sources are different from those of dust in local galaxies. There is recent evidence that the global dust emissivity index in local galaxies (β) is close to two. If β is closer to one in high-redshift SMSs, this would be a natural explanation of the low values of the flux ratio.

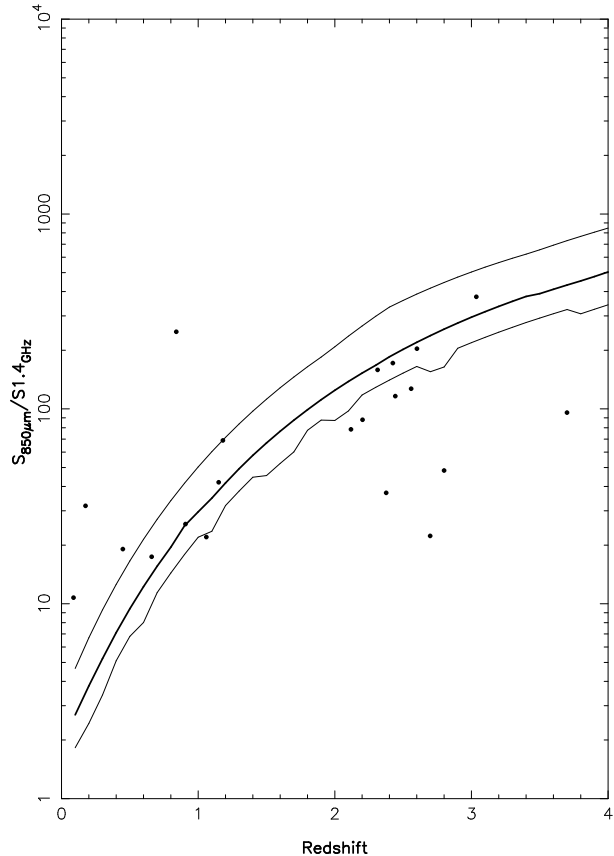


Figure 5. The ratio of $850\mu\text{m}$ flux to 1.4-GHz flux versus redshift. The lines show predictions based on the sample of low-redshift star-forming galaxies of Dunne et al. (2000). We used the SED of each galaxy to predict how the submillimetre to radio ratio should depend on redshift. The thick line shows the median prediction at each redshift, the thin lines show quasi- $\pm 1\sigma$ predictions based on the range of predicted values at each redshift (see Dunne, Clements and Eales 2000). The points show SMSs with spectroscopic redshifts and radio detections. The data are from Eales et al. (2000), Smail et al. (2000), Ivison et al. (2002), Chapman et al. (2002, 2003), Simpson et al. (2003), Clements et al. (2003).

7 THE COSMIC EVOLUTION OF DUST—A STATISTICAL APPROACH

In this section we assess the statistical evidence that the low values of the $850/1200\mu\text{m}$ flux ratio imply there is a significant population of SMSs at very high redshift (We assume that the low values are due to high redshifts rather than to a difference in the properties of dust, an assumption which may of course be wrong). Since the errors on the redshift estimates for the individual sources are so large, it is necessary to consider the sample as a whole. We have adopted the Monte-Carlo approach of generating artificial samples of sources on the assumption that there are no high-redshift SMSs, and then testing this assumption by comparing the flux ratios of the artificial samples with the flux ratios of the real sample. The Monte-Carlo approach allows us to include the effect on our artificial samples of the noise in the SCUBA and MAMBO observations.

In this Monte-Carlo simulation, we have made the standard assumption that the luminosity function of SMSs can

Table 3. Redshift Estimates

(1) Name	(2) z_{est} radio	(3) z_{est} 1200 μ m/850 μ m
LH-MM13	2.35 ^{+0.71} _{-0.64}	3.05 ^{+5.72} _{-3.05}
LH-MM34	2.85 ^{+1.0} _{-0.86}	1.35 ^{+5.61} _{-1.35}
LH-MM8	3.45 ^{+1.61} _{-0.78}	2.65 ^{+6.11} _{-2.65}
LH-MM86	2.55 ^{+0.72} _{-0.45}	0.45 ^{+2.60} _{-0.45}
NTT-MM3	2.05 ^{+0.67} _{-0.42}	4.25 ^{+∞} _{-4.25}
NTT-MM34 ^a	> 2.25
NTT-MM25	> 2.85	3.65 ^{+4.26} _{-2.53}
NTT-MM5	> 3.15	12.75 ^{+∞} _{-8.63}
NTT-MM1	2.45 ^{+0.64} _{-0.67}	> 8.95
NTT-MM16	2.25 ^{+0.85} _{-0.64}	6.35 ^{+∞} _{-4.85}
NTT-MM31	3.45 ^{+1.3} _{-1.03}	5.25 ^{+6.14} _{-1.93}
A2125-MM2	1.25 ^{+0.51} _{-0.22}	10.35 ^{+∞} _{-6.04}
A2125-MM11	1.75 ^{+0.54} _{-0.36}	> 9.65
A2125-MM13	2.05 ^{+0.64} _{-0.72}	1.55 ^{+5.11} _{-1.55}
A2125-MM21	2.45 ^{+0.67} _{-0.67}	3.95 ^{+8.44} _{-2.83}
A2125-MM26	2.25 ^{+0.63} _{-0.51}	1.85 ^{+1.92} _{-1.61}
A2125-MM27	2.45 ^{+0.63} _{-0.51}	< 1.0
A2125-MM28	0.55 ^{+0.22} _{-0.28}	3.45 ^{+∞} _{-3.45}
A2125-MM42	1.55 ^{+0.51} _{-0.36}	> 3.65
A2125-MM50	3.15 ^{+0.85} _{-1.0}	10.15 ^{+∞} _{-8.10}
A2125-MM32	2.25 ^{+0.67} _{-0.57}	9.85 ^{+∞} _{-7.53}

(1) Galaxy name. A letter as a superscript indicates there is a note on this source below; (2) redshift estimate from the ratio of the 1.4-GHz and 1200 μ m fluxes using the method described in the text; (3) redshift estimate from the 850 μ m and 1200 μ m fluxes, using the method described in the text.

Notes: a—the absence of a redshift estimate indicates that we could not obtain a satisfactory fit to the data at any redshift with any of the templates.

be factorised into its dependence on luminosity and on redshift: $\Phi(L, z) = E(z)\phi(L)$. We have to make four assumptions: (1) an assumption about the form of $E(z)$; (2) an assumption about the form of $\phi(L)$; (3) a cosmological model; (4) an assumption about the SEDs of SMSs. The first assumption, of course, is what we are really trying to test. Here, as we are only interested in whether there is any evidence for a high-redshift population of SMSs, we can make some simplifying assumptions. We have first assumed that there are no SMSs at $z < 1$. This is demonstrably not true (e.g. Chapman et al. 2003; Webb et al. 2003), but the vast majority of SMSs do appear to be beyond this redshift. The assumption is also a conservative one because without it the artificial samples would contain more high values of the $S_{850\mu\text{m}}/S_{1200\mu\text{m}}$ flux ratio. Above this redshift, we have assumed that $E(z)$ is independent of redshift up to a maximum redshift, z_{max} . By comparing the observed flux ratios with the artificial flux ratios for different values of z_{max} , we can address the question of whether there is a population of high-redshift SMSs.

The number of sources expected in a sample of sources with fluxes above a flux limit, S_{min} , as a function of redshift (the selection function) is given by:

$$n(z) = E(z) \int_{L(S_{min}, z)}^{\infty} \phi(L) dL \frac{dV}{dz}.$$

In this equation V is the comoving volume. $L(S_{min}, z)$ is the minimum luminosity an SMS could have at a redshift z and

still be detected in the sample. This quantity is very weakly dependent on redshift, and so the precise form of $\phi(L)$ has little effect on $n(z)$. We assumed that $\phi(L)$ has the same power-law form as the differential source counts: $\phi(L) \propto L^{-\alpha}$. We used 2.6 as our standard value of α , which was the value found by Bertoldi et al. (2001) for the 1200 μ m source counts. We tried different values of α but, as expected, it made almost no difference to the final results.

It is also necessary to make an assumption about the typical SED of an SMS, in order to calculate the lower limit of the integral. We used two extreme SEDs from the sample of IRAS galaxies of Dunne et al. (2000). NGC 958 is a galaxy whose SED is dominated by cold dust. The observed fluxes of this galaxy are fitted well by the two-component dust model of Dunne and Eales (2001), with dust at 20K and 44K in the ratio by mass of 186:1. At the other extreme is the galaxy IR1525+36, which, in the Dunne and Eales model, has dust at 19K and 45K in the ratio by mass of 15:1.

The first step in the simulation was to generate 40000 SMSs. The equation above is effectively a redshift probability distribution, and we used a random generator to produce a redshift for each SMS. We then used the luminosity function (the same used in the calculation of the selection function) and a random number generator to produce a luminosity for the source. From the luminosity and redshift of each SMS and the cosmological model we calculated the flux of the SMS. We produced SMSs with fluxes well below those which would have been detected in the MAMBO survey to

allow for the possibility of noise boosting the SMS into the survey. We carried out a separate simulation for each of the two SEDs.

The next step was to add the effects of observational noise. We first used a random number generator to add on gaussian noise to the $1200\mu\text{m}$ flux of each SMS, with a level similar to the noise in the real MAMBO survey. After eliminating the SMSs which would have fallen below the flux limit of the real MAMBO survey, we produced 1000 samples of SMSs, each of 21 sources. We then used the same SED we had used to calculate the selection function to calculate the $850\mu\text{m}$ source of each SMS, and then used a random number generator to add on gaussian noise similar to the noise of the SCUBA photometry.

Figure 6 shows the values of the $S_{850\mu\text{m}}/S_{1200\mu\text{m}}$ flux ratio for the real sample and the distributions predicted by two simulations, both with $z_{\text{max}} = 3$. In one simulation we have used the hot SED and in one the cold SED. The observed distribution appears quite different from the results of both simulations, a difference which is statistically significant (one-sample KS test) at $\ll 1\%$ level in both cases. Therefore, if the low values of the $S_{850\mu\text{m}}/S_{1200\mu\text{m}}$ flux ratio are caused by the effect of redshift, there is strong statistical evidence that the MAMBO samples contain a significant number of SMSs at $z > 3$.

8 DISCUSSION

The two possible explanations of our observational results are either that the dust emissivity index is low in the SMSs or that the SMSs are at extremely high redshifts. Both possibilities have interesting implications.

Although extragalactic submillimetre astronomers usually make the convenient assumption that the emissivity of dust is a universal constant (James et al. 2002), there is now plenty of evidence that it varies from place to place even within the Galaxy (e.g. Stepnik et al. 2003). As well as evidence for the variation of the emissivity at a particular wavelength, there is also evidence that the dust emissivity index varies. Dupac et al. (2002), for example, have used data taken with the balloon-borne submillimetre telescope PRONAOS to show that the dust emissivity index appears to depend inversely on dust temperature, decreasing to a value close to one in the hot parts of star-formation regions. Moreover, models of the evolution of dust in prestellar cores predict that the emissivity index should decrease in regions of increased density (Ossenkopf and Henning 1994). Therefore, although there is evidence that the dust emissivity index for the emission from galaxies as a whole is close to two at low redshifts (Dunne and Eales 2001; Amure 2003), it would not be surprising, in the possibly quite different conditions in the interstellar medium of SMSs, if the emissivity index were close to one.

The alternative explanation is that a significant fraction of the MAMBO sources lie at very high redshifts. There are two interesting points here. First, if SMSs are ellipticals being seen during the formation process, our result is more in line with the traditional model in which ellipticals form at early times in a distinct ‘epoch of galaxy formation’ (e.g. Larson 1975), rather than the current paradigm that ellipticals form by hierarchical merging over a long period of

cosmic time. The second interesting point is the constraint on the process that forms the dust. Some of our redshift estimates are as high as ten, when the time since the Big Bang is only 0.42 Gyr in the concordance model ($\Omega_M = 0.3$, $\Omega_\Lambda = 0.7$). Given the shortness of time, it is difficult to see how the dust in these objects could have been made in the atmospheres of evolved stars (Morgan and Edmunds 2003), and one is forced to assume that supernovae are the source of the dust.

9 CONCLUSIONS

We have observed 23 sources from the MAMBO $1200\mu\text{m}$ survey with SCUBA at $850\mu\text{m}$, detecting 19 of the sources. The sources generally have low values for the ratio of $850\mu\text{m}$ to $1200\mu\text{m}$ flux. At face value, the low values of the flux ratio imply very high redshifts, with 15 of the MAMBO sources having estimated redshifts > 3 . Redshifts estimated using the ratio of radio to submillimetre flux are, however, much lower. If the latter estimates are correct, the most likely explanation of the low values of the $850/1200\mu\text{m}$ flux ratio is that the global properties of the dust in high-redshift SMSs are different from those of dust in local galaxies. There is recent evidence that the global dust emissivity index in local galaxies (β) is close to two. If β is closer to one in high-redshift SMSs, this would be a natural explanation of the low values of the flux ratio.

ACKNOWLEDGMENTS

Stephen Eales thanks the Leverhulme Trust for the award of a research fellowship. We thank Phil Maukopf, Haley Morgan and Robert Priddey for useful conversations and Andrew Blain for many useful comments on the paper. The Institute for Radioastronomy at Millimeter Wavelengths (IRAM) is funded by the German Max-Planck-Society, the French CNRS, and the Spanish National Geographical Institute. The James Clerk Maxwell Telescope is operated by the Joint Astronomy Center on behalf of the UK Particle Physics and Astronomy Research Council, the Netherlands Organization for Scientific Research and the Canadian National Research Council. The National Radio Astronomy Observatory (NRAO) is operated by Associated Universities, Inc. under a cooperative agreement with the National Science Foundation.

REFERENCES

- Almaini, O. et al. 2003, MNRAS, 339, 397.
- Amure, M. 2003, Ph.D. thesis, Cardiff University.
- Barger, A.J. et al. 1998, Nature, 394, 428.
- Benford, D.J., Cox, P., Omont, A., Phillips, T. & McMahon, R. 1999, ApJ, 518, L65.
- Bertoldi, F. et al. 2000, A & A, 360, 92.
- Bertoldi, F., Menten, K.M. Kreysa, E., Carilli, C.L. & Owen, F. 2001, 24th meeting of the IAU, Joint Discussion 9, Manchester, England (astro-ph 0010553).
- Bertoldi, F. et al. 2003, in preparation.
- Blain, A.W., Kneib, J.-P., Ivison, R.J. & Smail, I. 1999, MNRAS, 512, 87.
- Blain, A.W. 1999, MNRAS, 309, 955.

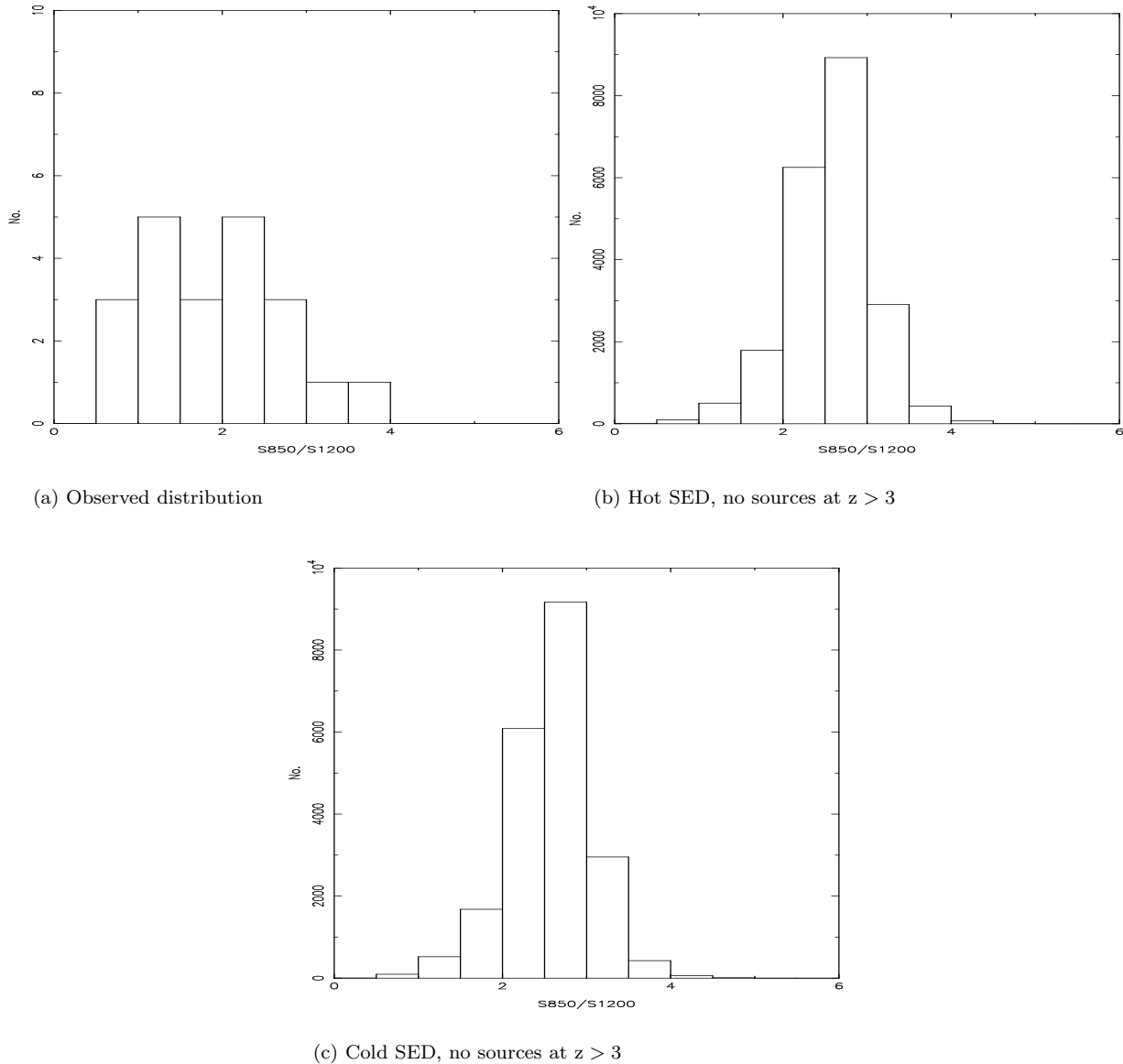


Figure 6. A comparison of the observed and predicted distributions of the $S_{850\mu\text{m}}/S_{1200\mu\text{m}}$ flux ratio. Figure 6(a) shows the distribution for the real sample. The other two figures show the predictions of models in which there are no SMSs at $z > 3$. In both models we have assumed the ‘concordance universe’ with $\Omega_M = 0.3$, $\Omega_\Lambda = 0.7$. In Figure 6(b) we have assumed the hot SED, in Figure 6(c) we have assumed the cold SED.

Blain, A.W., Barnard, V.E. & Chapman, S.C. 2003, MNRAS, 338, 733.
 Carilli, C.L. & Yun, M.S. 1999, ApJ, 513, L13.
 Carilli, C.L. & Yun, M.S. 2000, ApJ, 530, 618.
 Carilli, C.L. et al. 2001, ApJ, 555, 625.
 Chapman, S.C., Smail, I., Ivison, R.J., Helou, G., Dale, D.A. & Lagache, G. 2002, ApJ, 573, 66.
 Chapman, S.C. et al. 2003, Nature, in press.
 Clements, D. et al., in preparation.
 Dannebauer, H., Lehnert, M.D., Lutz, D., Tacconi, L., Bertoldi, F., Carilli, C., Genzel, R. & Menten, K. 2002, ApJ, 573, 473.
 Dey, A., Graham, J.R., Ivison, R.J., Smail, I., Wright, G.S. & Liu, M.C. 1999, ApJ, 519, 610.
 Dunne, L., Clements, D. & Eales, S. 2000, MNRAS, 319, 813.
 Dunne, L., Eales, S., Edmunds, M., Ivison, R., Alexander, P. & Clements, D. 2000, MNRAS, 315, 115.

Dunne, L. & Eales, S. 2001, MNRAS, 327, 697.
 Dunne, L., Eales, S. & Edmunds, M. 2003, MNRAS, in press (astro-ph 0210260).
 Dupac, X. et al. 2002, A & A, 392, 691.
 Eales, S.A., Lilly, S., Gear, W., Dunne, L., Bond, J.R., Hammer, F., Le Fèvre, O. & Crampton, D. 1999, ApJ, 515, 518.
 Eales, S.A., Lilly, S., Webb, T., Dunne, L., Gear, W., Clements, D. & Yun, M. 2000, AJ, 120, 2244.
 Eales, S.A. & Edmunds, M. 1996, MNRAS, 280, 1167.
 Eddington, A.S. 1940, MNRAS, 100, 354.
 Efstathiou, A. & Rowan-Robinson, M. 2003, MNRAS, in press.
 Hogg, D.W. 2001, AJ, 121, 1207.
 Holland, W.S. et al. 1999, MNRAS, 303, 659.
 Hughes, D.H. et al. 1998, Nature, 394, 241.
 Isaak, K.G., Priddey, R.S., McMahon, R.G., Omont, A., Peroux, C., Sharp, R.G. & Withington, S. 2002, MNRAS, 329, 141.

- Ivison, R. et al. 2000, MNRAS, 315, 209.
- Ivison, R.J. et al. 2002, MNRAS, 337, 11.
- James, A., Dunne, L., Eales, S. & Edmunds, M.G. 2002, MNRAS, 335, 753.
- Jenness, T. 1997, SURF - SCUBA user reduction facility. *Startlink User Note 216.1*.
- Kreysa, E. et al. 1998, Proc. SPIE Vol. 3357, Advanced Technology MMW, Radio, and Terahertz Telescopes, ed. T.G. Phillips, p319-325.
- Larson, R.B. 1975, MNRAS, 173, 671.
- Lisenfeld, U., Thum, C., Neri, R. & Sievers, A. 2000, Memo on IRAM web site (www.iram.fr).
- Omont, A., Cox, P., Bertoldi, F., McMahon, R.G., Carilli, C. & Isaak, K.G. 2001, A & A, 374, 371.
- Ossenkopf, V. and Henning, T. 1994, A & A, 291, 943.
- Owen, F. et al. 2003, in preparation.
- Morgan, H. & Edmunds, M. 2003, MNRAS, in press.
- Priddey, R.S. & McMahon, R.G. 2002, MNRAS, 324, 17p.
- Rengarajan, T.N. & Takeuchi, T. 2001, PASJ, 53, 433.
- Richards, E.A. 2000, ApJ, 533, 611.
- Sandell, G. 1994, MNRAS, 271, 75.
- Scott, S. et al. 2002, MNRAS, 331, 817.
- Smail, I., Ivison, R.J. and Blain, A.W. 1997, ApJ, 490, L5.
- Smail, I., Ivison, R.J., Owen, F.N. Blain, A.W. & Kneib, J.-P. 2000, ApJ, 528, 612.
- Smail, I., Ivison, R.J., Blain, A.W. & Kneib, J.-P. 2002, MNRAS, 331, 495.
- Smail, I., Chapman, S.C., Ivison, R.J., Blain, A.W., Takata, T., Heckman, T.M., Dunlop, J.S. & Sekiguchi, K. 2003, submitted to MNRAS (astro-ph 0303128).
- Simpson, C. et al., in preparation.
- Stepnik, B. et al. 2003, A & A, 398, 551.
- Webb, T. et al. 2003, ApJ, 587, 41.
- Waskett, T. et al. 2003, MNRAS, in press (astro-ph 0301610).